Electronic Supplementary Material (ESI) for Journal of Materials Chemistry C.

Supplementary Information

Effect of slurry pH on the chemical mechanical planarization of carbon-doped $Ge_2Sb_2Te_5$ phase change material

Jia Zheng,[†,‡] Wencheng Fang,[†,‡] Chengxing Li,[†,‡] Weili Liu,[†] Sannian Song,[†] Zhitang Song,[*,†] and Xilin Zhou[*,†]

†*State Key Laboratory of Functional Materials for Informatics, Shanghai Institute of Microsystem and Information Technology, Chinese Academy of Sciences, Shanghai 200050, China.*

‡*University of Chinese Academy of Sciences, Beijing 100049, China.*

E-mail: ztsong@mail.sim.ac.cn; xilinzhou@mail.sim.ac.cn

1. XPS depth profile analysis of the static etching

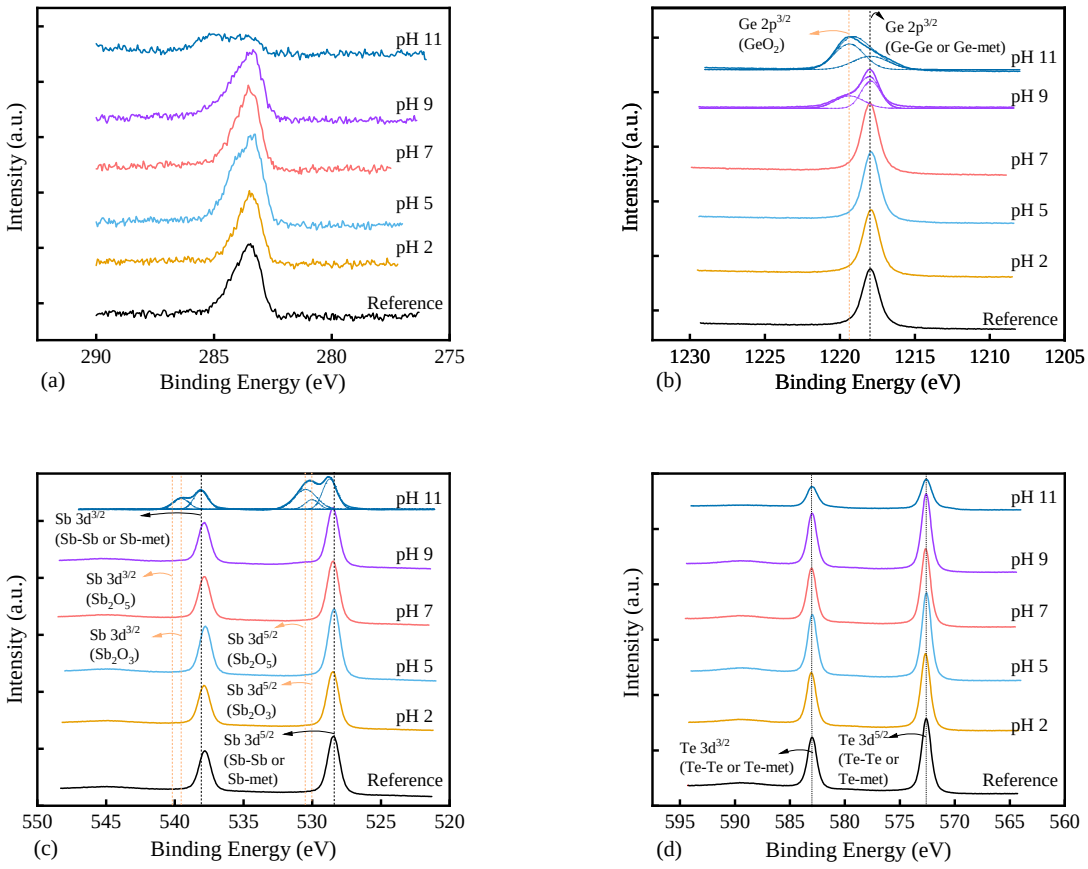

Fig. S 1: XPS depth profile of the static etching samples at slurry of pH 2, pH 5, pH 7, pH 9, and pH 11 after ion-etching 10 nm: (a) C 1s, (b) Ge 2p, (c) Sb 3d, and (d) Te 3d. Peaks of oxide states of all elements are marked as orange dot line.

Figure S1 shows the XPS depth profile of C 1s, Ge 2p, Sb 3d, and Te 3d of the static etching samples which were obtained by ion-etching 10 nm is shown in Figure S1 in the Supplementary Information. It is found that Te 3d remains metallic states for all static etching samples after ion-etching. The XPS peaks of germanium oxides were observed in the samples with a slurry of pH 9 and pH 11. By combining the surface morphologies after static etching test (see Figure 2), it is inferred that the corrosion reactions in the samples with a slurry of pH 9 and pH 11 have occurred up to 10 nm deep inside the C-GST film. From Figure S1(c) , the oxides state of Sb 3d was found in the sample with a slurry of pH 11. It

indicates the strongest corrosion in the C-GST surface when dipped in the slurry of pH 11. In the neutral and acid slurry, C-GST films undergoes moderate corrosion and oxidation as show in Figure S1.

2. XPS analysis of the C-GST films after CMP

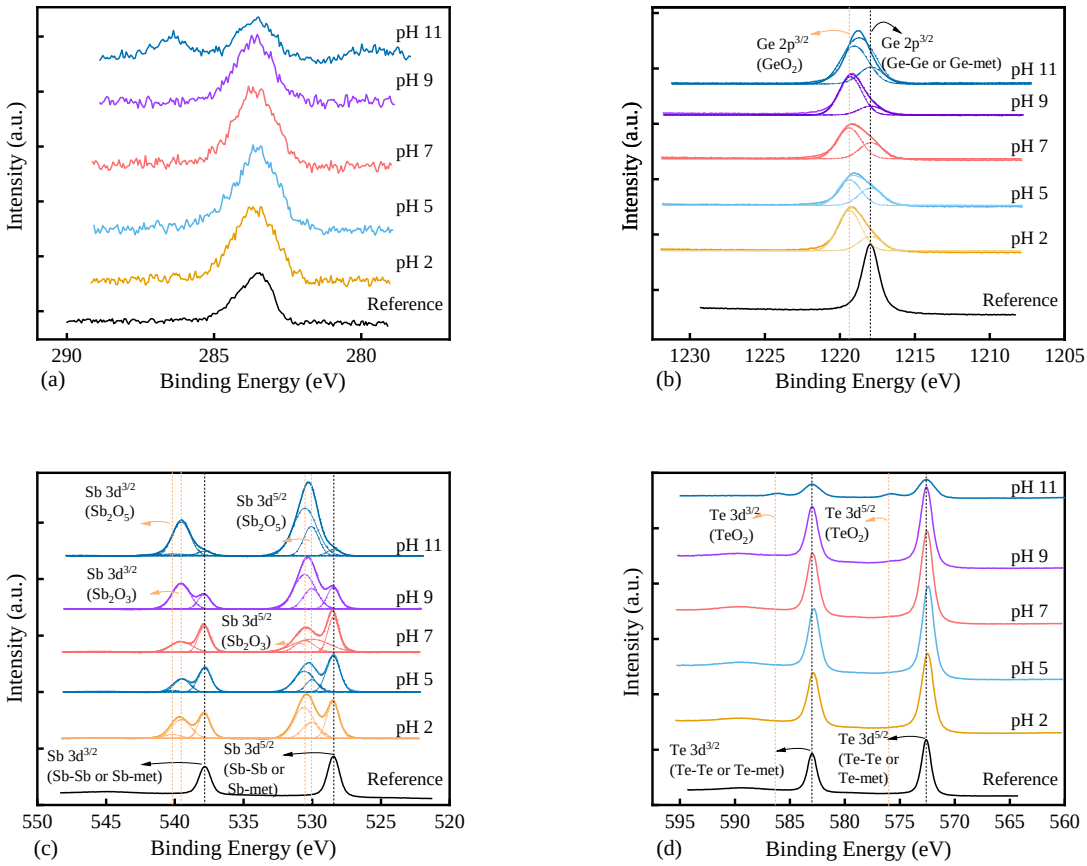

Fig. S 2: XPS spectra of the polished samples at slurry of pH 2, pH 5, pH 7, pH 9, and pH 11: (a) C 1s, (b) Ge 2p, (c) Sb 3d, and (d) Te 3d. Peaks of oxide states of all elements are marked as orange dot line.

Figure S2 shows the XPS results of C 1s, Ge $2p^3$, Sb 3d, and Te 3d of the polished samples in different slurry pH. The peaks of germanium and antimony oxides for the polished C-GST film are dominant while tellurium remains in metal state as shown in Figure S2(b), S2(c), and S2(d). This indicates Ge and Sb are more chemically reactive than Te. For the slurry of

pH 11, a small amount of tellurium oxide was observed, which indicating a strong corrosion in the film. For the slurry of pH 5 and pH 7, the metallic components of Sb 3d are dominant over the oxide components. For the other pH conditions, however, the peak intensity of the metallic Sb are decreased while the oxides peaks are stronger. It is known that oxides on the film surface are more likely to be removed by polishing. Compared to the XPS results of the static etching samples in the main manuscript (Figure 8), the metallic states of both Sb and Te were evident after chemical mechanical polishing as plotted in Figure S2(c) and S2(d).

3. TEM analysis of the C-GST films after CMP

Figure S3 shows the cross-sectional TEM images of the polished C-GST films. The Pt layer was deposited on the C-GST films to protect them from the ion damage during the fabrication of TEM samples. A smooth surface is evident in all samples on a relatively large scale. No obvious cracks are found on the surface of the C-GST films. A subsurface damage layer was observed in Figure S3(d), which is dependent significantly on the slurry pH.

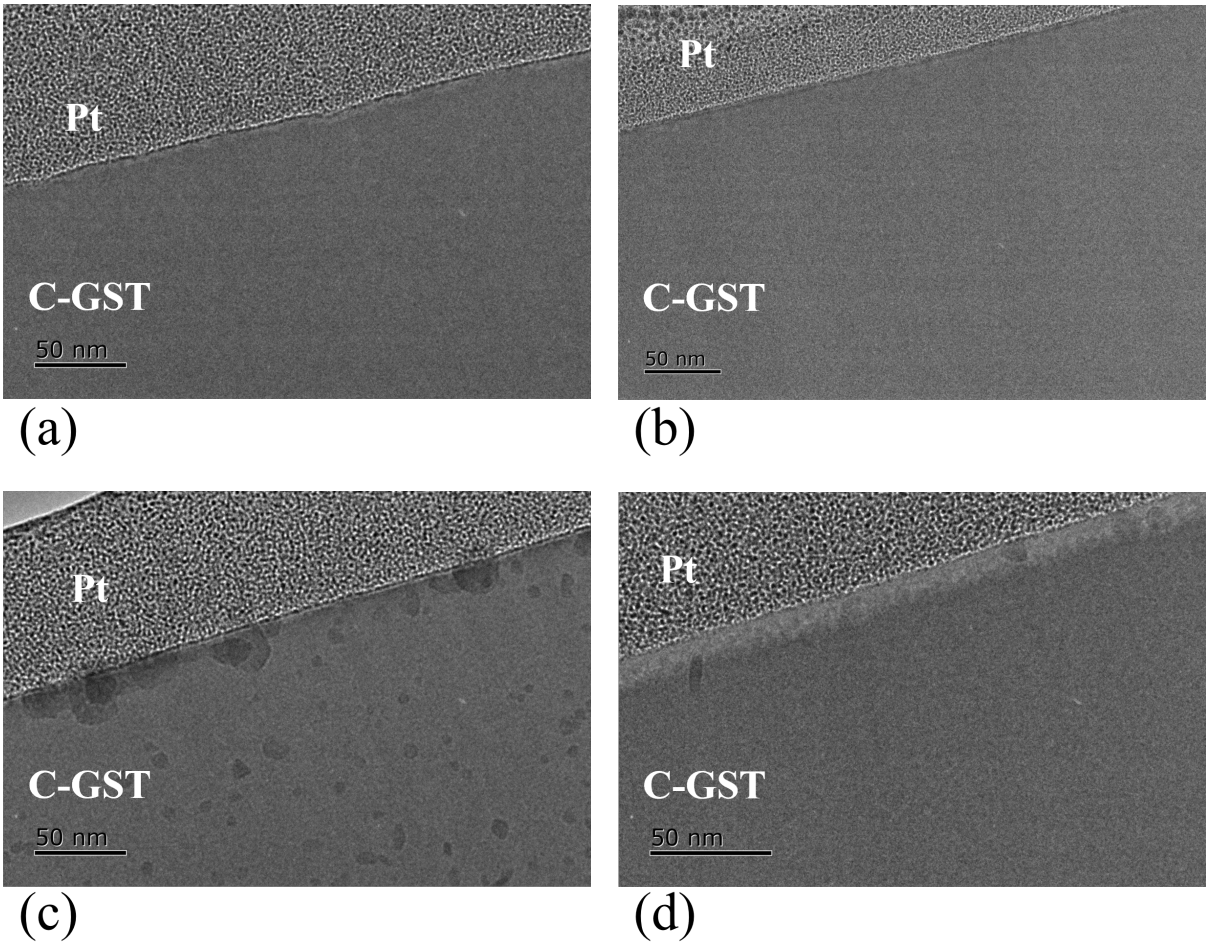

Fig. S 3: Cross-sectional TEM images of the C-GST films after polished in slurry of (a) pH 2, (b) pH 5, (c) pH 7, and (d) pH 11. The scale bar is 50 nm.